Breviscapine ameliorates CCl_4-induced liver injury in mice through inhibiting inflammatory apoptotic response and ROS generation

YU LIU, PEI-HAO WEN, XIN-XUE ZHANG, YANG DAI and QIANG HE

Department of Hepatobiliary Surgery, Beijing Chao-Yang Hospital
Affiliated to Capital University of Medical Science, Beijing 100000, P.R. China

Received May 28, 2017; Accepted April 5, 2018

DOI: 10.3892/ijmm.2018.3651

Abstract. Acute liver injury is characterized by fibrosis, inflammation and apoptosis, leading to liver failure, cirrhosis or cancer and affecting the clinical outcome in the long term. However, no effective therapeutic strategy is currently available. Breviscapine, a mixture of flavonoid glycosides, has been reported to have multiple biological functions. The present study aimed to investigate the effects of breviscapine on acute liver injury induced by CCl_4 in mice. C57BL/6 mice were subjected to intraperitoneal injection with CCl_4 for 8 weeks with or without breviscapine (15 or 30 mg/kg). Mice treated with CCl_4 developed acute liver injury, as evidenced by histological analysis, Masson trichrome and Sirius Red staining, accompanied with elevated levels of alanine aminotransferase and aspartate aminotransferase. Furthermore, increases in pro-inflammatory cytokines, chemokines and apoptotic factors, including caspase-3 and poly(ADP ribose) polymerase-2 (PARP-2), were observed. Breviscapine treatment significantly and dose-dependently reduced collagen deposition and the fibrotic area. Inflammatory cytokines were downregulated by breviscapine through inactivating Toll-like receptor 4/nuclear factor-κB signaling pathways. In addition, co-administration of breviscapine with CCl_4 decreased the apoptotic response by enhancing B-cell lymphoma-2 (Bcl-2) levels, while reducing Bcl-2-associated X protein, apoptotic protease activating factor 1, caspase-3 and PARP activity. Furthermore, CCl_4-induced oxidative stress was blocked by breviscapine through improving anti-oxidants and impeding mitogen-activated protein kinase pathways. The present study highlighted that breviscapine exhibited liver-protective effects against acute hepatic injury induced by CCl_4 via suppressing inflammation and apoptosis.

Correspondence to: Dr Qiang He, Department of Hepatobiliary Surgery, Beijing Chao-Yang Hospital Affiliated to Capital University of Medical Science, 8 Courtyard, Worker Palaestra South Road, Chaoyang, Beijing 100000, P.R. China
E-mail: heqiangbcyh@qq.com

Key words: liver injury, breviscapine, inflammation, apoptosis, oxidative stress

Introduction

The liver is known as the primary organ important for drug and chemical substance metabolism (1). Liver injury may be induced by drug abuse, viral infection and heavy alcohol consumption, and is considered to be a common clinical disease (2,3). CCl_4 is a well-known hepatotoxin, which may induce liver injury through various mechanisms, including oxidative stress, inflammatory response and apoptosis (4,5). The CCl_4-induced animal model of acute liver injury is well established, leading to fibrosis, inflammation and apoptotic response in mice (6). Previous studies have assessed the possible molecular mechanism of liver toxicity induced by CCl_4 (7,8). Certain hepatoprotective agents have been investigated and applied in clinical practice, but a large proportion of them have potential adverse effects (9,10). Therefore, application of natural products isolated from plants as an effective and safe therapeutic strategy for liver disease has been in the focus of recent research (11,12).

Breviscapine (Fig. 1A) is a mixture of flavonoid glycosides isolated from Chinese herbs, including *Erigerin breviscapus* (Vant.) (13). Breviscapine has been reported to have various biological activities, including anti-oxidant, anticancer, anti-degenerative and anti-angiogenesis effects (14-16). It has been indicated that breviscapine administration is safe and has low toxicity to various normal cell types (17,18). In addition, the anti-inflammatory effect of breviscapine has been reported (16). Accordingly, breviscapine is extensively used for the treatment of cerebrovascular diseases caused by cerebral infarction, hypertension and chronic arachnoiditis along with their sequelae, and is suggested to inhibit tumor proliferation and angiogenesis, thereby limiting tumor development (19). However, the effects of breviscapine on liver injury and the underlying molecular mechanisms still remain to be fully elucidated.

The present study attempted to investigate whether breviscapine may be effectively used as a therapeutic drug, and to test this, it was administered to mice with CCl_4-induced liver injury and L02 cells challenged with lipopolysaccharide (LPS).

It was indicated that inflammatory cytokines were down-regulated by breviscapine through inactivating the Toll-like receptor (TLR)4/nuclear factor (NF)-κB signaling pathways. Breviscapine co-administered with CCl_4 reduced apoptosis by inactivating the caspase-3 signaling pathway. In addition, CCl_4-induced oxidative stress was blocked by breviscapine through improving anti-oxidants and impeding mitogen-activated protein kinase (MAPK) signaling. The present study indicated that breviscapine exerted protective effects against acute liver injury by suppressing inflammation, apoptosis and oxidative stress, which may be used as a therapeutic strategy for patients with liver injury.

Materials and methods

Reagents. CCl_4 was obtained from Tianjin Baishi Chemical (Tianjin, China). A Cell Counting Kit-8 (CCK-8) was purchased from Beyotime Institute of Biotechnology (Shanghai, China). Breviscapine (purity, ≥98%) and Picrosirius red were purchased from Sigma-Aldrich (Merck KGaA, Darmstadt, Germany). Antibodies to B-cell lymphoma-2 (Bcl-2)-associated X protein (Bax; cat. no. 2772; 1:1,000 dilution), Bcl-2 (cat. no. 3498; 1:1,000 dilution), myeloid differentiation primary response gene 88 (MyD88; cat. no. 4283; 1:1,000 dilution), phospho (p)-NF-κB (cat. no. 3033; 1:1,000 dilution), NF-κB (cat. no. 8242; 1:1,000 dilution), phospho-inhibitor of NF-κB (p-IκBα; cat. no. 2859; 1:1,000 dilution), phospho-IκB kinase α (p-IKKα; cat. no. 2078; 1:1,000 dilution), extracellular signal-regulated kinase (ERK)1/2 (cat. no. 4377; 1:1,000 dilution) p-ERK1/2 (cat. no. 9101; 1:1,000 dilution), p38 (cat. no. 8690; 1:1,000 dilution), p-p38 (cat. no. 9215; 1:1,000 dilution), superoxide dismutase (SOD1; cat. no. 13141; 1:1,000 dilution) and GAPDH (cat. no. 5174; 1:1,000 dilution), all raised in rabbit, were obtained from Cell Signaling Technology Inc. (Danvers, MA, USA). Antibodies against TLR4 (cat. no. ab13556; 1:1,000 dilution), c-Jun N-terminal kinase (JNK; cat. no. ab4821; 1:1,000 dilution), p-JNK (cat. no. ab47337; 1:1,000 dilution), nuclear factor erythroid 2-related factor 2 (Nrf2; cat. no. ab62352; 1:1,000 dilution), heme oxygenase (HO)-1 (cat. no. ab13248; 1:1,000 dilution), NAD(P)H quinone dehydrogenase-1 (NQO-1; cat. no. ab34173, 1:1000 dilution) activated caspase-3 (cat. no. ab52293; 1:1,000 dilution), pro-caspase-3 (cat. no. ab90437; 1:1,000 dilution), cleaved poly(ADP ribose) polymerase (PARP; cat. no. ab13907; 1:1,000 dilution), PARP (cat. no. ab218132; 1:1,000 dilution) and apoptotic protease activating factor-1 (Apaf-1; cat. no. ab2000; 1:1,000 dilution), all raised in rabbit, were purchased from Abcam (Cambridge, MA, USA). A HRP-labelled secondary antibody (cat. no. KIT-5902; 1:200 dilution; Max Vision HRP-polymer anti-rabbit IHC kit) was purchased from Maxim BioTechnology Co., Ltd. (Fuzhou, China).

Animals and treatments. A total of 40 healthy male C57BL/6 mice (age, 6-8 weeks, weight, 20-22 g), were purchased from Shanghai Experimental Animal Center (Shanghai, China) and kept under standard conditions of 25±2˚C and 50±10% humidity with a 12-h light/dark cycle with food and water provided *ad libitum* in cages. The experimental protocols, which were in accordance with the Guide for the Care and Use of Experimental Animals of the National Institutes of Health (NIH) from 1996 (20) and were approved by the Institutional Animal Care and Use Committee of the Beijing Chao-Yang Hospital (Beijing, China). Prior to experimental treatment, all mice were kept under the standard conditions for 1 week for adaptation. Next, the mice were divided into four groups (n=10 each): i) Control group (Con); ii) CCl_4-treated model group (Mod); iii) CCl_4 and breviscapine co-treatment (15 mg/kg) and iv) CCl_4 and breviscapine co-treatment (30 mg/kg). A total of 30 mice were treated twice a week with 8 consecutive intraperitoneal (i.p.) injections of 1 ml/kg CCl_4 (diluted at 1:10 in olive oil) to induce liver fibrosis. As for the breviscapine-treated groups, 15 or 30 mg/kg breviscapine was administered to the mice each day by oral gavage (Fig. 1B) for 8 weeks. At the end of the experiment, blood samples and liver tissues were collected from the mice for further assays.

Cell culture and treatment. The L02 human normal liver cell line was purchased from KeyGEN BioTECH (Nanjing, China). The BRL-3A rat normal liver line and the AML-12 mouse normal liver cell line were all purchased from the cell bank of the Chinese Academy of Sciences (Shanghai, China). All cells were cultured and grown in Dulbecco's modified Eagle's medium supplemented with 10% heat-inactivated fetal bovine serum (both from Gibco; Thermo Fisher Scientific, Inc., Waltham, MA, USA), 100 U/ml penicillin and 100 mg/ml streptomycin at 37˚C in a humidified atmosphere containing 5% CO_2. The cells were then exposed to LPS (100 ng/ml) for 24 h in the absence or presence of breviscapine at different concentrations (20 and 40 μM) (21-24).

Cell viability assessment. L02 cells were seeded in a 96-well plate at $1x10^3$ cells/well overnight, prior to the addition of breviscapine. The cells were treated with various concentrations of breviscapine (0, 5, 10, 20 and 40 μM) for different durations ranging from 0-72 h (0, 6, 12, 24, 36, 48 and 72 h) in the absence of LPS. Subsequently, 10 μl CCK-8 solution (Dojindo Laboratories, Kumamoto, Japan) was added to each well and the plate was incubated at 37˚C for 1 h. Finally, the absorbance at 450 nm was measured to determine the cell viability. The protocol was performed according to the manufacturer's protocols.

Analysis of biochemical indicators. To evaluate liver injury, serum alanine aminotransferase (ALT) and aspartate aminotransferase (AST) levels were determined using ALT and AST reagent kits (Nanjing Jiancheng Bioengineering Institute, Nanjing, China) according to manufacturer's protocols. Albumin levels in the serum were measured by using an albumin reagent kit (NanJing JianCheng Bioengineering Institute). As for the hepatic hydroxyproline content, 200 mg Snap-frozen liver specimens were weighed and hydrolyzed in NaOH (2 M). The hydroxyproline content was quantified following the manufacturer's instructions of the hydroxyproline measurement kit (Nanjing Jiancheng Bioengineering Institute). SOD, glutathione (GSH), malondialdehyde (MDA), H_2O_2 and myeloperoxidase (MPO) levels were measured using the standard diagnostic kits purchased from NanJing JianCheng Bioengineering Institute.

ELISA. The levels of tumor necrosis factor (TNF)-α, interleukin (IL)-1β, IL-6 and monocyte chemoattractant protein (MCP)-1

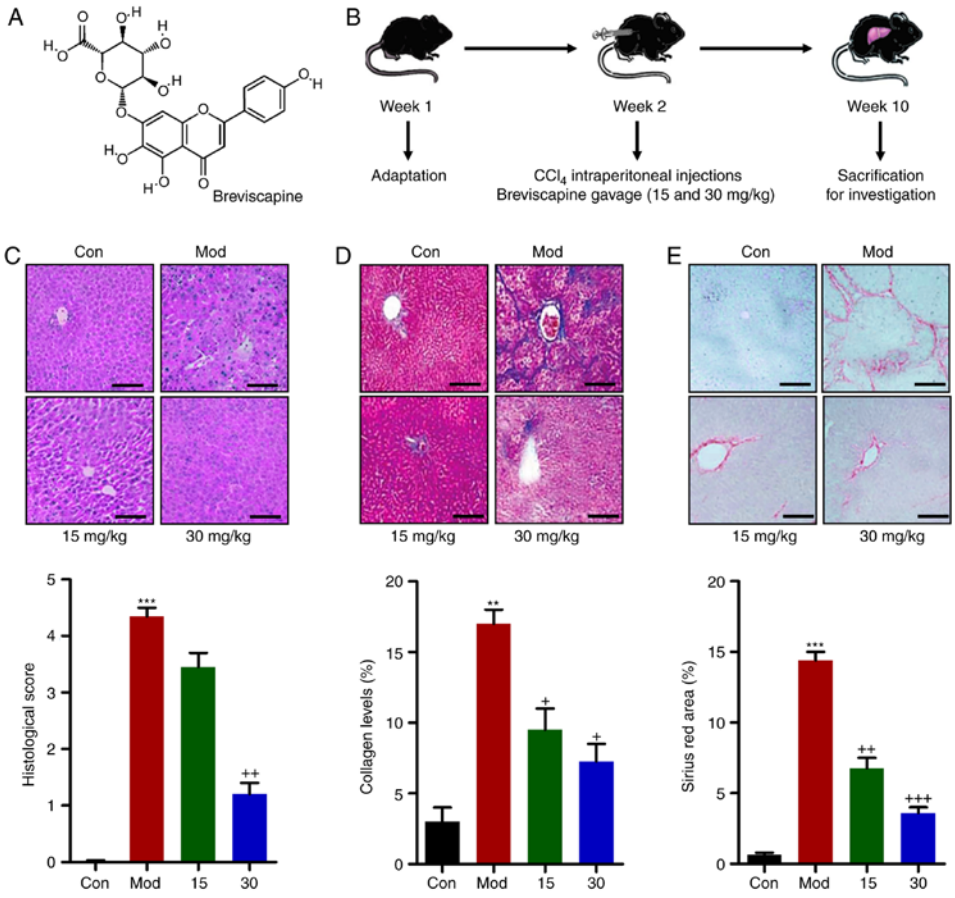

Figure 1. Breviscapine improves CCl_4-induced histological changes and collagen deposition in mouse livers. (A) Chemical structure of breviscapine. (B) Schematic of the study design. (C) Histological analysis of liver sections from CCl_4-induced mice by hematoxylin and eosin staining, and the histological score. (D) Masson analysis for the deposition of collagen was performed. (E) Collagen accumulation was measured by Picric acid-Sirius red staining. Representative images and quantification are displayed. Scale bar, 100 μm. Mean values are expressed as the mean ± standard error of the mean (n=10). **P<0.01 and ***P<0.001 vs. Con; $^{+}$P<0.05, $^{++}$P<0.01 and $^{+++}$P<0.001 vs. CCl_4-induced mice. Mod, CCl_4-treated group; Con, control group.

in serum and liver tissue samples were determined by using the ELISA kits purchased from R&D systems (Minneapolis, MN, USA) following the manufacturer's protocols.

Terminal deoxynucleotidyl transferase deoxyuridinetriphosphate nick end labelling (TUNEL) analysis. TUNEL analysis was used to indicate apoptosis in the liver tissue samples. The assay detects the 3' hydroxyl ends of DNA fragments. The staining was performed with the *In Situ* Cell Death Detection kit (TUNEL assay; KeyGen Biotech; Nanjing, China) following the manufacturer's protocols. Recombinant DNase I (Takara Biotechnology Co., Ltd., Dalian, China) was included in the positive control. The immunostained liver cells of were quantified using a light microscope and results are presented as a percentage of the control.

Assessment of reactive oxygen species (ROS) generation. A 5-μM intracellular probe of non-fluorescent 2',7'-dichlorofluorescein-diacetate (DCFH-DA; KeyGen Biotech) was used to detect the cellular ROS formation. The L02 cells ($5x10^5$ cells/well) were treated with LPS (100 ng/ml) with or without breviscapine for 24 h. DCFH-DA was then added and the cells were cultured continuously in the dark at 37˚C for 20 min. Subsequently, the fluorescent cells were visualized using a fluorescence microscope.

Immunofluorescent staining. For *in vivo* analysis, the frozen liver sections were blocked using a solution containing 4% normal goat serum (OriGene Technologies, Inc., Rockville, MD, USA), 1% Triton X-100 and 1% bovine serum albumin (Xi'an Guanyu Bio-Tech Co., Ltd., Xi'an, China) for 1 h at the room temperature. Next, the samples were incubated with anti-TLR4 primary antibody (1:100 dilution) at 4˚C overnight. Subsequently, they were washed three times with PBS (0.1 M) containing 0.5% Triton X-100 for 5 min each time, and the sections were then incubated with Alexa Fluor 594-labeled anti-rabbit secondary antibody (cat. no. A-11072, 1:500 dilution; Invitrogen; Thermo Fisher Scientific, Inc.) at room temperature for 1 h prior to analysis with a fluorescent microscope equipped with a digital camera. Finally, the fluorescent cells were quantified.

In vitro, the L02 cells were washed three times with chilled PBS and fixed with 3.7% (v/v) formaldehyde in PBS for 15 min. The specimens were then permeabilized for 5 min using 0.1% Triton X-100. For Apaf-1 fluorescence staining, 50 μg/ml mouse anti-Apaf-1 antibody was applied and incubated at 4˚C overnight, followed by staining with anti-mouse secondary antibody labelled with Alexa Fluor 488 (cat. no. A-21441; 1:500 dilution; Invitrogen; Thermo Fisher Scientific, Inc.) for 30 min. Subsequent to washing in PBS for 3 times, the immunofluorescence was visualized and quantified with a Zeiss

LSM 710 confocal laser system (Carl Zeiss AG, Oberkochen, Germany).

Immunohistological analysis. The liver tissue samples obtained from mice were fixed in 4% paraformaldehyde, embedded in paraffin, sectioned at 4 mm and then stained with haematoxylin and eosin (H&E) for 10 min or Masson's trichrome blue for 5 min at room temperature to analyze the liver injury and collagen deposition, respectively. The score of injured level was described in a previous study (25). The sections stained with Masson's trichrome were scanned and analyzed using a digital image analyzer (Image-Pro Analyzer 7 software; Media Cybernetics, Inc., Rockville, MD, USA). Sirius red staining was also used to calculate the fibrotic area. In brief, the liver sections were incubated with picrosirius red for 2 h at room temperature and then washed with acetic acid and water. The percentage of the fibrotic area was calculated in 5 randomly selected fields per slide. Furthermore, liver tissue samples were also subjected to immunohistochemical staining for the assessment of Bax and Apaf-1 expression. The sections were stained with rabbit anti-Bax (1:200 dilution) or rabbit anti-Apaf-1 (1:200 dilution) at 4˚C overnight. Slides were incubated in a humidified chamber for 1 h and incubated for 10 min with a HRP-labelled secondary antibody (Max Vision HRP-polymer anti-rabbit IHC kit, 1:200 dilution) at room temperature. Immunoreactive proteins were visualized using a DAB substrate (cat. no. SK-4100; Vector Laboratories, Inc., Burlingame, CA, USA), followed by counterstaining with hematoxylin at room temperature for 50 min. Immunohistochemical quantification was carried out using image analysis software (ImageJ; 1.46a; National Institutes of Health, Bethesda, MD, US). The histological protocol was in line with standard procedures (26,27).

Western blot analysis. The liver tissues and L02 cells were homogenized with 10% (wt/vol) hypotonic buffer (1 mM EDTA, 1 mM Pefabloc SC (Roche Applied Science, Penzberg, Germany), 5 μg/ml leupeptin, 25 mM Tris-HCl, 5 μg/ml soybean trypsin inhibitor (Sigma-Aldrich; Merck KGaA), 4 mM benzamidine and 50 μg/ml aprotinin; pH 8.0). The final supernatants were obtained by centrifugation at 12,000 x g rpm for 20 min. The protein concentration was determined using a bicinchoninic acid protein assay kit (Thermo Fisher Scientific, Inc.) with bovine serum albumin as a standard. Equal amounts (20-40 μg) of total protein were subjected to 10 or 12% SDS-PAGE and electrophoretically transferred to the polyvinylidene difluoride membranes (Merck KGaA). The membranes were then blocked with 5% skim milk Tris buffered saline with 0.1% Tween-20 (TBST), washed, and then incubated with primary antibodies (Bax, Bcl-2, MyD88, p-NF-κB, NF-κB, p-IκBα, p-IKKα, ERK1/2, p-ERK1/2, p38, p-p38, SOD1, GAPDH, TLR4, JNK, p-JNK, Nrf2, HO-1, NQO-1, activated caspase-3, pro-caspase-3, PARP, Apaf-1) overnight at 4˚C. Then, the membrane was washed with TBST three times, followed by incubation with a horseradish peroxidase (HRP)-conjugated secondary antibody (cat. no. ab191866; 1:2,500 dilution; Abcam) at room temperature for 2 h. Western blot bands were observed using a GE Healthcare ECL Western Blotting Analysis System (GE Healthcare, Little Chalfont, UK) and exposed to X-ray film (Eastman Kodak, Rochester NY, USA). For enhanced chemiluminescence, detection reagents A and B was mixed at a 1:1 ratio, which was immediately added to the blotting membrane. In total, 0.125 ml working solution was used per cm^2 for each membrane. The blot was incubated for 1 min at room temperature and excess reagents were drained. The blot was then exposed to X-ray film. The protein expression levels were defined as the grey value determined with ImageJ software version 1.4.2b (NIH, Bethesda, MD, USA) and standardized by presenting them as a fold of the housekeeping gene GAPDH as the control.

Reverse transcription-quantitative polymerase chain reaction (RT-qPCR). Total RNA was extracted from tissues and cells with the TRI Reagent (Sigma-Aldrich; Merck KGaA) following the manufacturer's instructions and treated with deoxyribonuclease I (Roche Applied Science). The mRNA was then reverse transcribed to complementary DNA using the miScript II RT kit (Qiagen, Hilden, Germany), which was then amplified and quantified by real-time qPCR using All-in-One qPCR Mix (GeneCopoeia, Inc., Rockville, MD, USA) in a 20 ml reaction volume containing 10 ml of 2X All-in-One qPCR Mix (GeneCopoeia, Inc.), 1 μl of 2 μM forward primer, 1 μl of 2 μM reverse primer, 1 μl of cDNA, and 6 μl of nuclease-free water. The thermocycling conditions were for 35 cycles of 95˚C for 20 sec, 54˚C for 30 sec and 72˚C for 30 sec according to a previous study (28). Fold changes in mRNA levels of target genes relative to the endogenous control GAPDH were calculated. In brief, the Cq method was used for quantification cycle values of each target gene were subtracted from the Ct values of the housekeeping gene GAPDH (ΔCt). Target gene ΔΔCt was calculated as ΔCt of the target gene minus the ΔCt of the control. The fold change in mRNA expression was calculated as $2^{-\Delta\Delta Cq}$ (29). The primer sequences (5'-3') were as follows: TNF-α forward, CAAGAG AGTAGGGAAGTGG and reverse, AGCAGAACGCCGACT AGCTAAC; IL-1β forward, AGAAAGATAGCAGGTACGC and reverse, CGTTCTAGAACTATTGGAGC; IL-6 forward, GAGAGCCGACGGTGAGAC and reverse, CGAGAATGA AGAGGCACACT; IL-18 forward, TGACTAGAGAGCGCA GTCAAC and reverse, TGCTCAAGGCAAGTGTAATTCC; Bcl-2 forward, GATGGATCATGACACAGGACA and reverse, TCAACAGCCTAGAGATTATGTG; Bax forward, AACAGA GACATAAGGCGGCTAC and reverse, CATCACCTAGGA GGTGGCTTAT; Apaf-1 forward, TCGGTAAGAGCTCAA GAGCC and reverse, TCTGCAACTTCAAGGCGTGCAA; GAPDH forward, AGGAACGCAGTTCGCATCGCAA and reverse, TCACACCTACAGCCAACACGA.

Statistical analysis. Values are expressed as the mean ± standard error of the mean. Statistical analyses were performed using GraphPad Prism version 6.0 (Graph Pad Software, Inc., La Jolla, CA, USA). Analysis of variance followed by Dunnett's least-significant differences post-hoc test was performed for comparison between groups. $P<0.05$ was considered to indicate a statistically significant difference.

Results

Breviscapine improves CCl_4-induced histological changes and collagen deposition in mice. CCl_4 is well-known to cause hepatic injury, apoptosis and necrosis (4,5). In order to investigate the

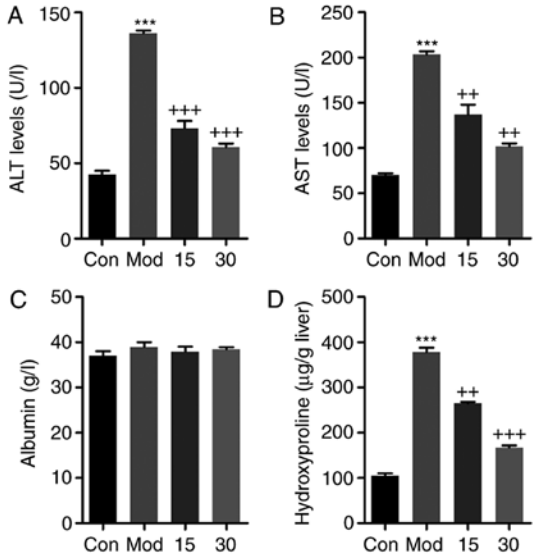

Figure 2. Breviscapine attenuates liver injury in mice induced by CCl_4. (A) ALT, (B) AST and (C) Albumin levels in the serum of mice were examined to assess the effect of breviscapine in regulating liver injury induced by CCl_4. (D) Liver hydroxyproline levels were assessed. Values are expressed as the mean ± standard error of the mean (n=10). ***P<0.001 vs. Con; $^{++}$P<0.01 and $^{+++}$P<0.001 vs. CCl_4-induced mice. Mod, CCl_4-treated group; Con, control group; ALT, alanine aminotransferase; AST, aspartate aminotransferase.

effects of breviscapine on hepatic damage, male mice were subjected to a 8-week treatment with CCl_4 with optional co-treatment with 15 or 30 mg/kg breviscapine. H&E staining indicated that CCl_4 treatment produced liver injury, resulting in higher histological score compared with those in the control group. Of note, breviscapine administration ameliorated liver injury induced by CCl_4, resulting in lower histological score compared with those in the Mod group (Fig. 1C). In addition, CCl_4 treatment generated higher collagen accumulation, as indicated by Masson trichrome staining, which was reduced by breviscapine administration (Fig. 1D). Finally, Sirius Red staining indicated that marked fibrosis occurred in the CCl_4 treated-group. However, breviscapine reduced the fibrotic area in the liver tissue of CCl_4-induced mice (Fig. 1E). These results indicated that breviscapine administration significantly attenuated CCl_4-induced liver damage.

Breviscapine attenuates liver injury in mice induced by CCl_4. To further clarify the therapeutic effect of breviscapine on liver injury induced by CCl_4, serum ALT, AST, albumin and liver hydroxyproline were calculated. As presented in Fig. 2A and B, respectively, ALT and AST levels in the serum were markedly elevated in the CCl_4-group compared with those in the control group, while breviscapine significantly decreased the ALT and AST levels in a dose-dependent manner. As for albumin, no significant difference was observed among the four groups (Fig. 2C). Furthermore, hydroxyproline levels in the in liver were markedly increased after CCl_4 treatment. However, breviscapine administration reduced the hydroxyproline levels in comparison to those in the CCl_4-treated group (Fig. 2D). These results indicated that breviscapine had preventive effects against liver injury caused by CCl_4 treatment.

Breviscapine ameliorates CCl_4-induced liver injury by reducing pro-inflammatory cytokine secretion. The levels of TNF-α, IL-6, IL-1β and MCP-1 in the liver tissues were also elevated after CCl_4 treatment, which was inhibited by breviscapine administration, as determined by ELISA (Fig. 3A). In addition, the circulating pro-inflammatory cytokines TNF-α, IL-6 and IL-1β, as well as the chemokine MCP-1, were assessed

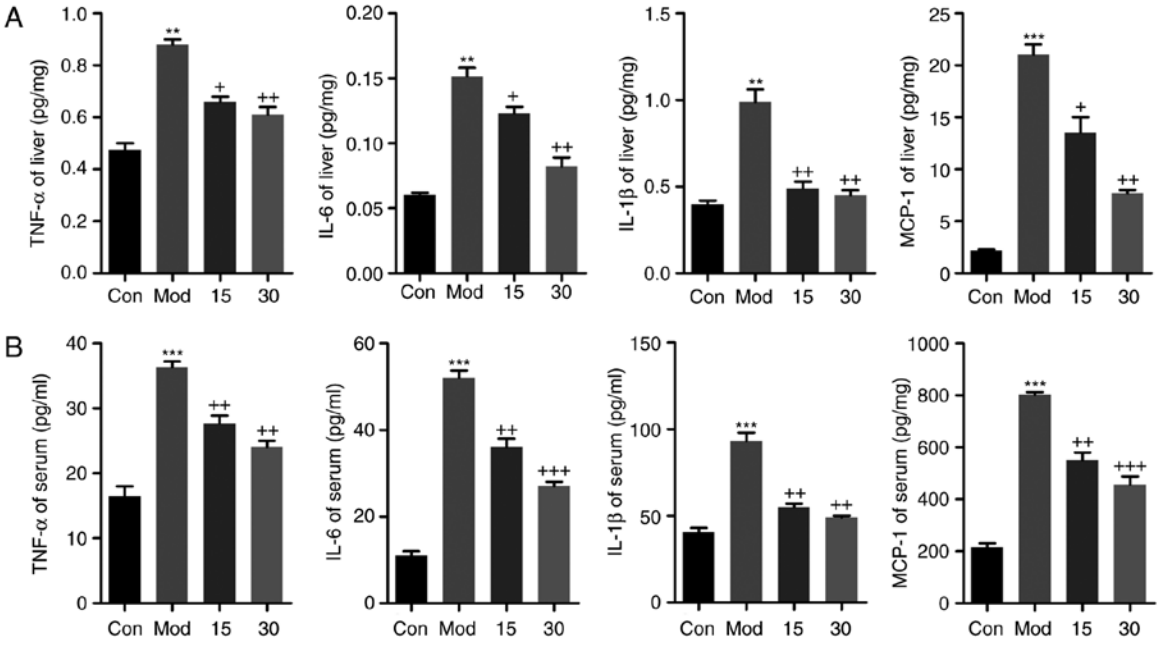

Figure 3. Breviscapine ameliorates CCl_4-induced liver injury by reducing pro-inflammatory cytokine secretion. (A) Serum pro-inflammatory cytokines TNF-α, IL-6 and IL-1β and chemokine of MCP-1 were determined using ELISA kits. (B) Liver pro-inflammatory cytokines TNF-α, IL-6 and IL-1β and chemokine MCP-1 were determined using commercial ELISA kits. Values are expressed as the mean ± standard error of the mean (n=10). **P<0.01 and ***P<0.001 vs. Con; $^{+}$P<0.05, $^{++}$P<0.01 and $^{+++}$P<0.001 vs. CCl_4-induced mice. Mod, CCl_4-treated group; Con, control group; TNF, tumor necrosis factor; IL, interleukin; MCP, monocyte chemoattractant protein.

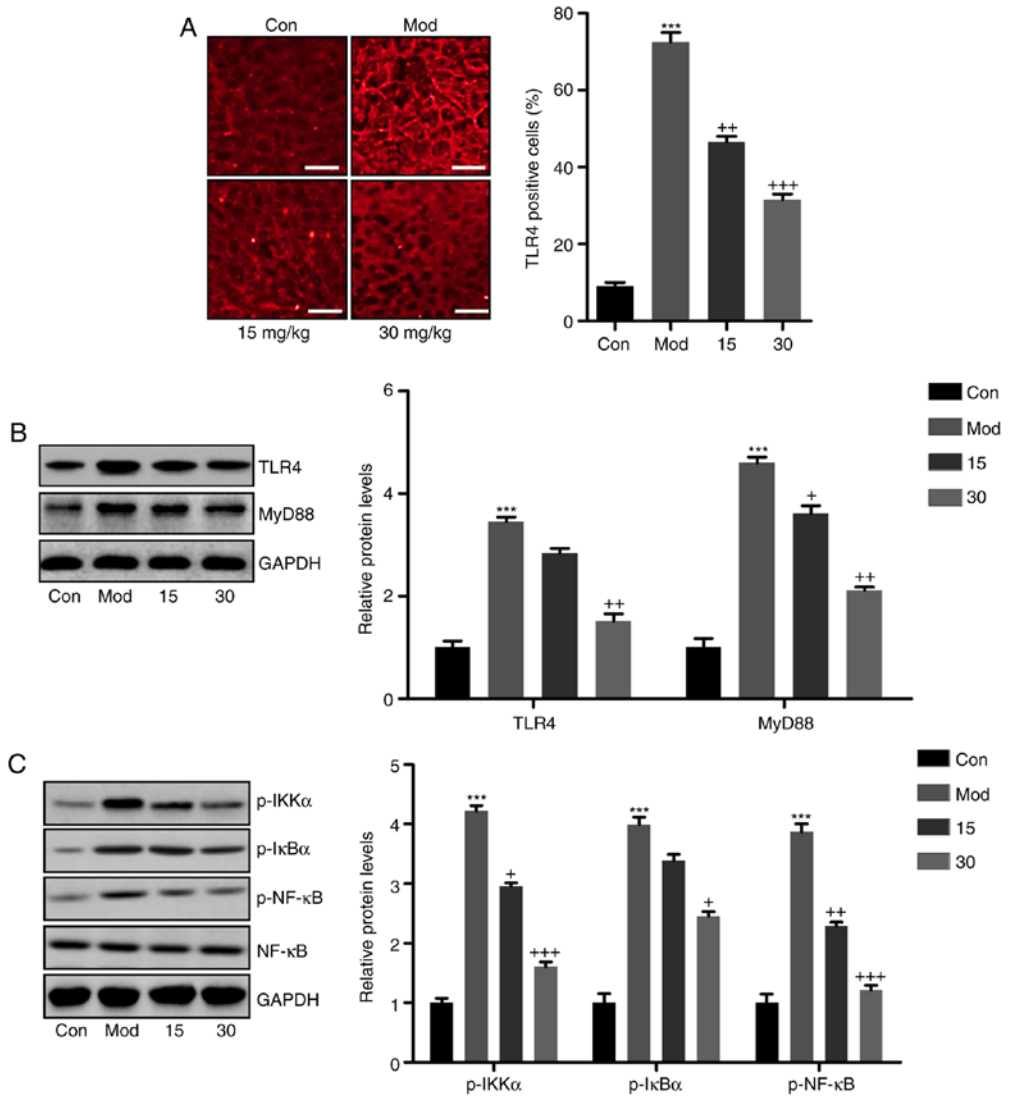

Figure 4. Breviscapine ameliorates CCl_4-induced liver injury by via suppression of TLR4/NF-κB signaling. (A) Immunofluorescence microscopy was performed to explore the TLR4 intensity in the liver sections of mice after CCl_4 induction. Scale bar, 100 μm. (B) TLR4 and MyD88 protein levels were calculated by western blot analysis, displayed with the representative images and quantified levels. (C) Phosphorylated IKKα, IκBα and NF-κB levels were determined by immunoblot analysis. The quantified levels were also displayed. Values are expressed as the mean ± standard error of the mean (n=10). ***P<0.001 vs. Con; $^{+}$P<0.05, $^{++}$P<0.01 and $^{+++}$P<0.001 vs. CCl_4-induced mice. Mod, CCl_4-treated group; Con, control group; TLR, Toll-like receptor; p-NF-κB, phosphorylated nuclear factor κB; IκBα, inhibitor of NF-κB; IKKα, IκB kinase α; MyD88, myeloid differentiation primary response gene 88.

by ELISA (Fig. 3B). Compared with those in the control group, the serum levels of TNF-α, IL-6, IL-1β and MCP-1 were markedly elevated in the CCl_4-treated group. However, mice treated with breviscapine exhibited a significant downregulation of TNF-α, IL-6, IL-1β and MCP-1 levels in the serum. Taken together, the results indicated that breviscapine suppressed the secretion of pro-inflammatory cytokines and chemokines in serum and their expression in liver tissues.

The attenuation of CCl_4-induced liver injury by breviscapine proceeds via suppression of TLR4/NF-κB signaling. According to previous studies, TLR4 is involved in liver injury induced by CCl_4, initiating the inflammatory response by stimulating NF-κB activity (30). To determine whether breviscapine exerted its protective effects against CCl_4-induced liver injury by suppressing inflammation via TLR4/NF-κB signaling, immunofluorescence and western blot analyses were used to determine the expression of TLR4 and NF-κB pathway components. Immunofluorescence staining indicated that TLR4 was significantly upregulated in the liver tissue samples of mice induced with CCl_4, when compared with those in the control group (Fig. 4A). The number TLR4-positive cells was markedly decreased in breviscapine-treated mice, when compared with that in the CCl_4 group. To further explore the mechanistic involvement of the TLR4 signaling pathway, TLR4 and its downstream signaling molecule MyD88 were assessed by western blot analysis. As presented in Fig. 4B, a significant increase in TLR4 and MyD88 expression levels was observed in the CCl_4 vs. the control group. However, breviscapine-treated mice exhibited reduced TLR4 and MyD88 protein levels compared with those in the CCl_4 group. Next, the NF-κB signaling pathway was examined. As indicated in Fig. 4C, mice subjected to CCl_4 treatment had higher levels of phosphorylated IKKα and IκBα levels in comparison with those in the control group, accompanied with significantly higher level of phosphorylated NF-κB. Of note, IKKα, IκBα and NF-κB

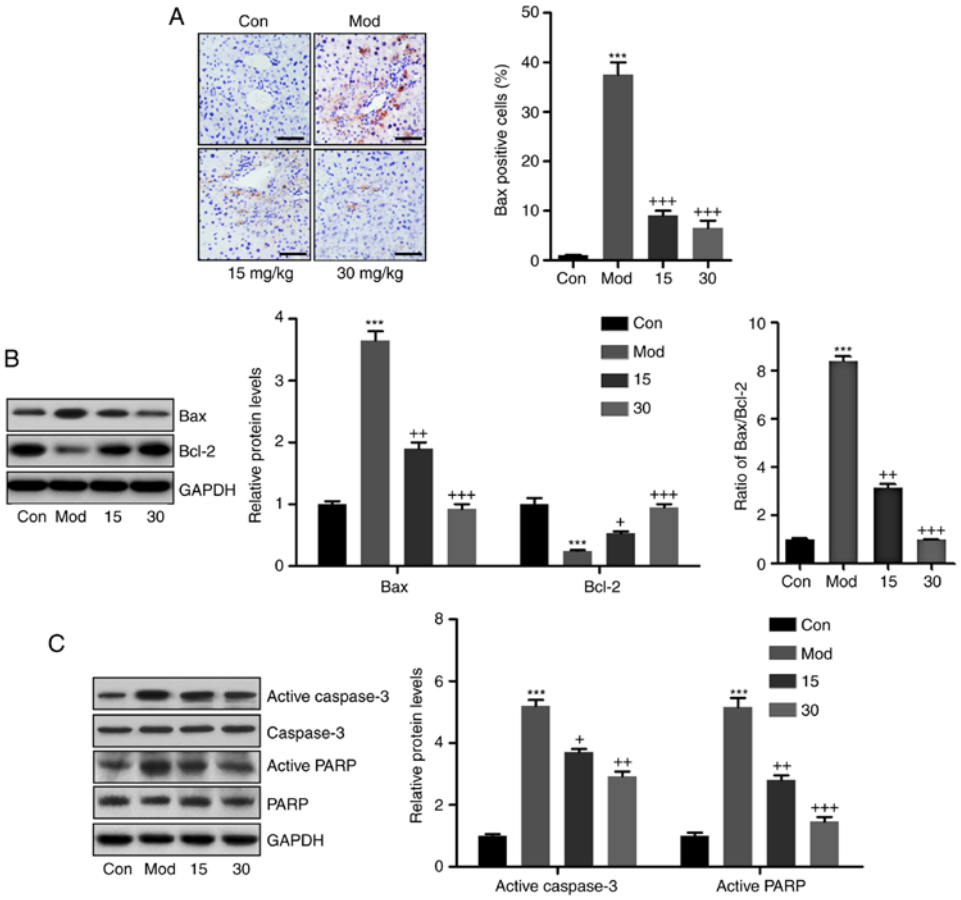

Figure 5. Breviscapine attenuates liver injury by inhibiting apoptosis in CCl_4-induced mice. (A) Immunohistochemical assays were performed to evaluate Bax levels in the liver sections of mice subjected to different treatments. Scale bar, 100 μm. (B) Bax and Bcl-2 protein levels were evaluated by western blot analysis. Quantified levels of Bax and Bcl-2 are displayed, and the ratio of Bax/Bcl-2 was exhibited. (C) Active caspase-3 and PARP-1 protein abundance was determined by western blot analysis. Representative blot images of proteins are displayed, accompanied with the quantified levels. Values are expressed as the mean ± standard error of the mean (n=10). ***P<0.001 vs. Con; $^{+}$P<0.05, $^{++}$P<0.01 and $^{+++}$P<0.001 vs. CCl_4-induced mice. Mod, CCl_4-treated group; Con, control group; Bcl-2, B-cell lymphoma-2; Bax, Bcl-2-associated X protein; PARP, poly(ADP ribose) polymerase.

activation were downregulated in breviscapine-treated mice subjected to CCl_4 treatment, compared with those in mice only treated with CCl_4. In conclusion, the results demonstrated that breviscapine administration de-activated the TLR4/NF-κB signaling pathway in CCl_4-treated mice.

Breviscapine attenuates liver injury by inhibiting apoptosis in CCl_4-induced mice. To determine whether CCl_4 caused apoptosis, the expression levels of apoptosis-associated molecules were determined. CCl_4 treatment markedly increased the mRNA levels of the pro-apoptotic mitochondrial protein Bax, which was decreased when the mice were co-treated with breviscapine (Fig. 5A). In addition, western blot analysis indicated that the expression levels of the anti-apoptotic molecule Bcl-2 exhibited an opposite trend to that of the protein expression levels of Bax in the CCl_4-treated mice, indicating that CCl_4 induced apoptosis in the liver tissue samples. Of note, breviscapine treatment caused a significant upregulation of Bcl-2 expression to prevent apoptosis (Fig. 5B). Finally, casapse-3 and PARP were determined by western blot to further clarify the role of breviscapine in CCl_4-induced apoptosis. As presented in Fig. 5C, active caspase-3 and PARP were increased in the CCl_4-treated group in comparison with the control group, while breviscapine had a suppressive effect on caspase-3 and PARP cleavage.

In addition, TUNEL analysis was performed to further evaluate cellular apoptosis. The representative images and the histogram in Fig. 6A confirmed that CCl_4 induced massive apoptosis, while breviscapine administration significantly reduced the amount of TUNEL-positive cells. Apaf-1 is important during caspase-dependent mitochondrial apoptosis (31). As indicated in Fig. 6B, Apaf-1 was significantly upregulated following CCl_4 treatment, while breviscapine administration reduced Apaf-1 protein levels to inhibit apoptosis. These results indicated that breviscapine attenuated CCl_4-induced liver injury by suppressing the apoptotic response.

Breviscapine reduces oxidative stress in the livers of mice treated with CCl_4. Oxidative stress is another essential factor contributing to acute liver injury (32,33). Thus, the present study further explored whether breviscapine modulates oxidative stress to attenuate liver injury induced by CCl_4 *in vivo*. As presented in Fig. 7A, liver tissue samples of mice from the CCl_4 group exhibited reduced levels of the anti-oxidants SOD and GSH, which were comparable to those in the Con group. Breviscapine significantly upregulated SOD activity and GSH levels in liver tissues. By contrast, MDA and H_2O_2 levels were enhanced by CCl_4 treatment, but were downregulated after breviscapine administration. Furthermore, western

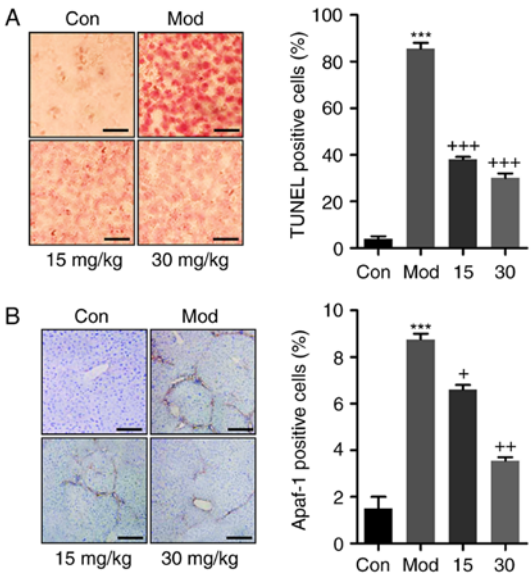

Figure 6. Breviscapine reduces apoptosis the liver of mice treated with CCl_4. (A) TUNEL analysis was used to assess apoptosis in CCl_4-induced livers in mice after Breviscapine administration. Scale bar, 100 μm. (B) Apaf-1 positive cells were calculated in the liver sections of mice. Scale bar, 100 μm. Values are expressed as the mean ± standard error of the mean (n=10). ***P<0.001 vs. Con; $^{+}$P<0.05, $^{++}$P<0.01 and $^{+++}$P<0.001 vs. CCl_4-induced mice. Mod, CCl_4-treated group; Con, control group; Apaf-1, apoptotic protease activating factor 1; TUNEL, terminal deoxynucleotidyl transferase deoxyuridinetriphosphate nick end labelling.

blot analysis indicated that the CCl_4-induced decrease of anti-oxidants, including SOD1, HO-1, NQO-1 and Nrf2, was inhibited by treatment with breviscapine (Fig. 7B). MAPK signaling is closely associated with the progression of oxidative stress (34,35). The ratios of phosphorylated p38, ERK1/2 and JNK vs. total proteins are shown. As presented in Fig. 7C, p38, ERK1/2 and JNK were phosphorylated by CCl_4 stimulation, and breviscapine inhibited the activation of these MAPKs. Therefore, the above results indicated that breviscapine reduced oxidative stress to alleviate liver injury induced by CCl_4.

Breviscapine downregulates the LPS-induced inflammatory response in L02 cells in vitro. In order to further confirm the effects of breviscapine on liver injury, an *in vitro* experiment was performed. First, the viability of liver cell lines was examined by CCK-8 analysis. As presented in Fig. 8A, the normal liver cell lines L02, BRL-3A and AML-12 were treated with various concentrations of breviscapine (0, 5, 10, 20 and 40 μM) for different durations ranging from 0-72 h. The cell viability assay indicated that the above treatment had almost no significant effect on normal liver cell lines, except for the BRL-3A cells treated with breviscapine at 40 μM for 72 h. Therefore, it was suggested that breviscapine is safe for application, exerting only little cytotoxicity to normal liver cell lines isolated from a human, rat and mouse. In the next experiment, L02 cells were treated with 100 ng/ml LPS for 24 h, in

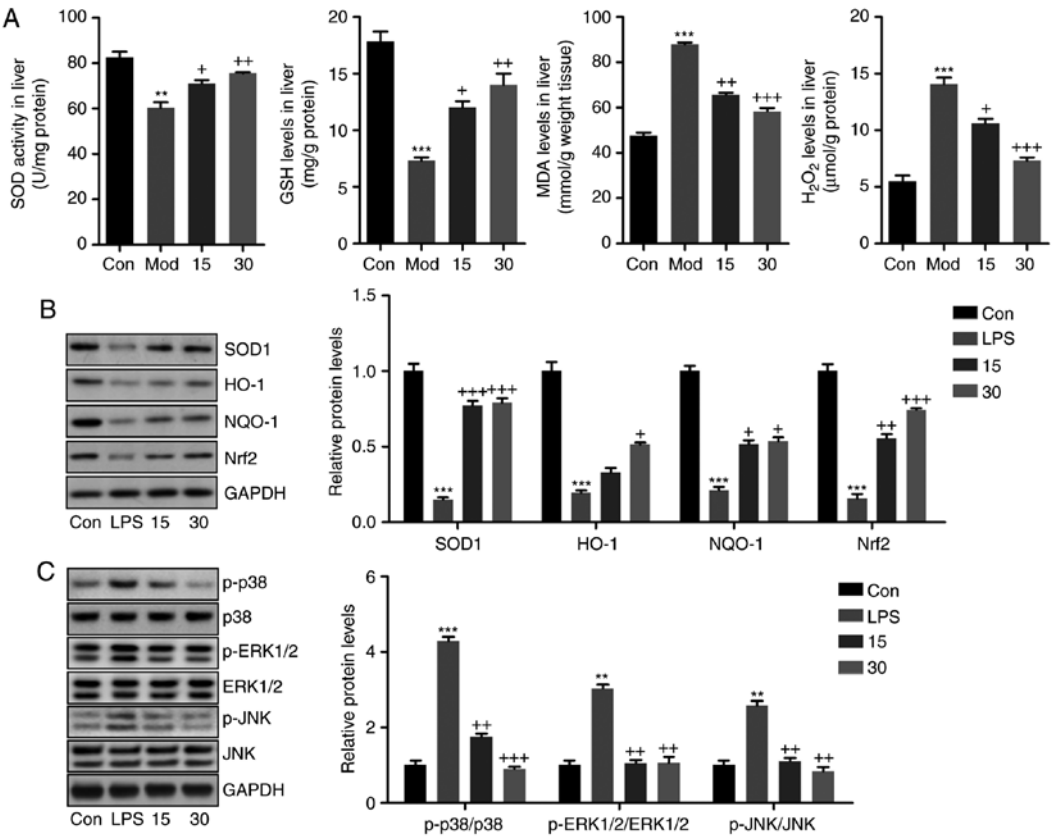

Figure 7. Breviscapine reduces oxidative stress in the livers of mice induced with CCl_4. (A) Liver SOD activity, GSH levels, MDA levels and H_2O_2 levels were measured. (B) Western blot analysis was used to determine SOD1, NQO-1, HO-1 and Nrf2 protein expression levels in the liver tissue samples. (C) p-p38, p-ERK1/2 and p-JNK protein levels in liver samples were calculated using western blot assays. Values are expressed as the mean ± standard error of the mean (n=8). **P<0.01 and ***P<0.001 vs. Con; $^{+}$P<0.05, $^{++}$P<0.01 and $^{+++}$P<0.001 vs. CCl_4-induced mice. Mod, CCl_4-treated group; Con, control group. SOD, superoxide dismutase; GSH, glutathione synthase; MDA, malondialdehyde; HO-1, heme oxygenase 1; NQO-1, NAD(P)H quinone dehydrogenase 1; p-ERK, phosphorylated extracellular signal-regulated kinase; JNK, c-Jun N-terminal kinase; Nrf2, nuclear factor erythroid 2-related factor 2.

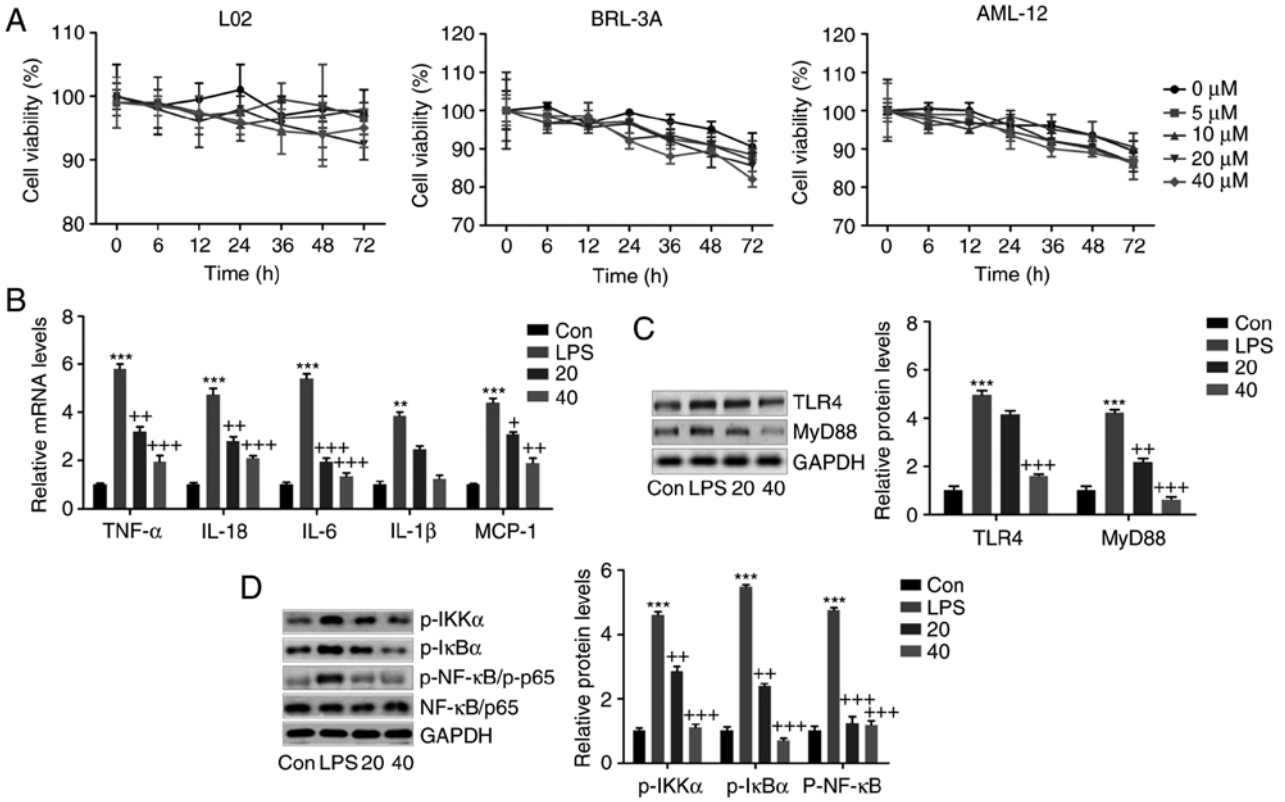

Figure 8. Breviscapine suppresses the inflammatory response in L02 cells stimulated with LPS *in vitro*. (A) The normal liver cell lines of L02, BRL-3A and AML-12 were treated with breviscapine at different concentrations (0, 5, 10, 20 and 40 μM) for various durations ranging from 0-72 h. The cell viability was measured by a cell counting kit-8 assay to evaluate the cytotoxicity of breviscapine to liver cells. In addition, L02 cells were exposed to 100 ng/ml LPS for 24 h in the absence or presence of breviscapine (20 or 40 μM). (B) The pro-inflammatory cytokines TNF-α, IL-6, IL-1β and IL-18, and the chemokine MCP-1 were assessed by reverse transcription-quantitative polymerase chain reaction analysis. (C) Western blot analysis was used to evaluate TLR4 and MyD88 levels in L02 cells after various treatments. (D) IKKα, IκBα and NF-κB (p65) phosphorylation were examined by immunoblotting analysis. Representative western blot images and quantified protein levels are provided. Values are expressed as the mean ± standard error of the mean (n=8). *P<0.05, **P<0.01 and ***P<0.001 vs. Con; $^{+}$P<0.05, $^{++}$P<0.01 and $^{+++}$P<0.001 vs. LPS group. LPS, lipopolysaccharide; Con, control group; p-NF-κB, phosphorylated nuclear factor-κB; IκBα, inhibitor of NF-κB; IKKα, IκB kinase α; TLR, Toll-like receptor; MyD88, myeloid differentiation primary response gene 88; TNF, tumor necrosis factor; IL, interleukin; MCP, monocyte chemoattractant protein.

the presence or absence of breviscapine at 20 or 40 μM. The pro-inflammatory cytokines TNF-α, IL-6, IL-1β and IL-18, and the chemokine MCP-1 were highly induced by LPS at the mRNA level, as indicated by RT-qPCR analysis. Breviscapine co-treatment reduced the mRNA levels of these factors, indicating that breviscapine exerted anti-inflammatory effects on liver cells (Fig. 8B). LPS markedly increased the protein levels of TLR4 and MyD88, which was markedly inhibited by breviscapine (Fig. 8C). In addition, LPS-induced increases in the levels of phosphorylated IKKα, IκBα and NF-κB (p65) protein were suppressed by breviscapine, as indicated by western blot analysis (Fig. 8D). The above evidence indicated that breviscapine ameliorated the inflammatory response through attenuating the activation of TLR4/NF-κB signaling.

Breviscapine reduces LPS-induced apoptosis of L02 cells. In L02 cells subjected to various treatments, apoptotic markers were assessed. RT-qPCR and western blot analysis indicated that LPS induced decreases in the mRNA and protein levels of the anti-apoptotic molecule Bcl-2, which was inhibited by breviscapine in a dose-dependent manner (Fig. 9A and B). By contrast, the mRNA and protein expression levels of Bax and Apaf-1 were increased in the LPS-treated group, which was inhibited by co-treatment with breviscapine (Fig. 9A and B). In addition, western blot analysis indicated that the cleavage of caspase-3 and PARP was significantly induced by LPS, when compared with that in the control group. Of note, breviscapine co-treatment reduced caspase-3 and PARP activity in a dose-dependent manner, which was in line with the *in vivo* results (Fig. 9C). Finally, immunofluorescence analysis indicated that LPS-induced Apaf-1 expression in L02 cells was attenuated by breviscapine treatment (Fig. 9D). The above results demonstrated that breviscapine ameliorated apoptosis in LPS-induced L02 cells to attenuate liver injury.

Breviscapine reduces LPS-induced oxidative stress in L02 cells. *In vivo*, breviscapine exerted anti-oxidant effects to attenuate CCl_4-induced liver injury. A further *in vitro* experiment was performed to confirm this result. As presented in Fig. 10A, the DCFH-DA assay revealed that LPS treatment induced massive ROS generation, which was inhibited by breviscapine. In addition, breviscapine restored the levels of SOD1, NQO-1, HO-1 and Nrf2, which were decreased in LPS-treated cells (Fig. 10B). However, phosphorylation of p38, ERK1/2 and JNK stimulated by LPS was markedly reduced by breviscapine in a dose-dependent manner (Fig. 10C). These results further confirmed that breviscapine exerted protective effects against liver injury through inhibiting ROS production.

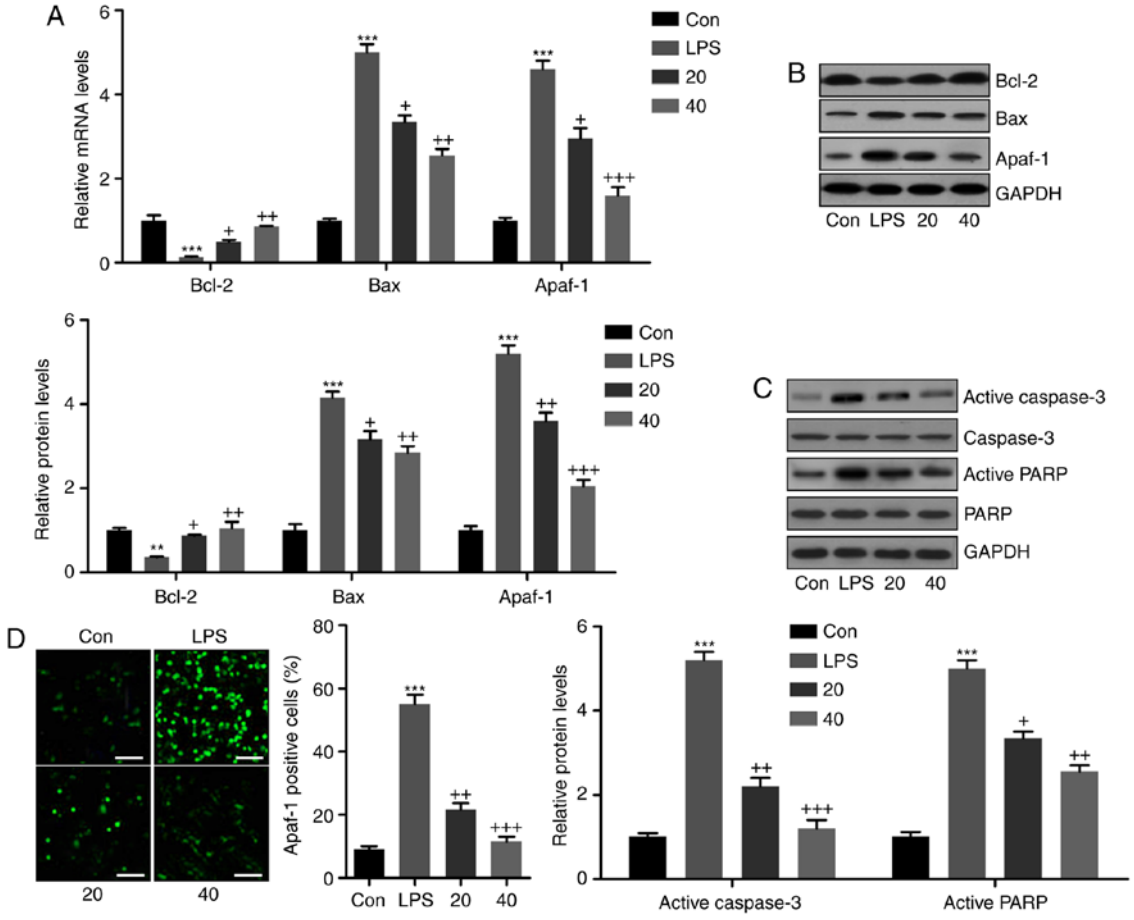

Figure 9. Breviscapine reduces LPS-induced apoptosis in L02 cells. (A) Reverse transcription-quantitative polymerase chain reaction analysis was used to determine the levels of Bcl-2, Bax and Apaf-1 in LPS-treated L02 cells in the presence or absence of breviscapine. (B) Western blot analysis was performed to determine Bcl-2, Bax and Apaf-1 expression at the protein level. Representative western blot images and quantified protein levels are provided. (C) Apaf-1 positive cells were examined by immunofluorescence analysis among L02 cells exposed to LPS with or without breviscapine treatment (20 or 40 μM). Scale bar, 50 μm. (D) Active caspase-3 and PARP protein levels were assessed by western blot analysis. Representative western blot images and quantified protein levels are provided. Values are expressed as the mean ± standard error of the mean (n=10). **P<0.01 and ***P<0.001 vs. Con; $^{+}$P<0.05, $^{++}$P<0.01 and $^{+++}$P<0.001 vs. LPS group. Con, control; Bcl-2; B-cell lymphoma-2; Bax, Bcl-2-associated X protein; PARP, poly(ADP ribose) polymerase; Apaf-1, apoptotic protease activating factor 1; LPS, lipopolysaccharide.

Discussion

The liver is an essential organ, which is involved in a variety of activities, including the generation of blood clotting factors, bile acid secretion, destruction of bacteria in the blood and detoxification. Liver injury may be triggered by various factors, including microbes, drugs and xenobiotics, as well as metabolites in the liver (1-3,36). Previous studies have indicated that breviscapine has beneficial properties, such as anti-oxidant, anticancer and anti-degenerative effects (14-16). While breviscapine has been investigated in various diseases, the current knowledge regarding its protective effect against liver injury induced by CCl_4 is limited, and further study is required to elucidate the underlying mechanism. In the present study, histological analysis indicated that breviscapine attenuated CCl_4-induced liver cell injury. Masson staining further demonstrated that the collagen deposition caused by CCl_4 was significantly decreased by breviscapine. In addition, the fibrotic area caused by CCl_4 was reduced by breviscapine administration. Supplementation with breviscapine in CCl_4-induced mice attenuated liver injury, reduced fibrosis and improved hepatic function by reducing the CCl_4-associated increases in ALT and AST levels, which was in line with previous studies (37,38).

To identify the possible molecular mechanisms, including the signaling pathways involved, the inflammatory response was investigated. The inflammatory response has been reported as a pivotal process leading to organ injury under various stresses (39,40). As previously described, CCl_4 treatment induced acute liver injury, which was closely associated with inflammation by elevating pro-inflammatory cytokine secretion (41). In line with previous studies, the present study confirmed that the pro-inflammatory cytokines IL-1β, TNF-α, IL-18 and IL-6 were highly expressed in CCl_4-treated mice *in vivo*, as well as in LPS-induced L02 cells *in vitro*, which represents a major mechanism of liver injury. Of note, breviscapine administration significantly reduced the release of these cytokines, suggesting its role in ameliorating CCl_4-induced liver injury. The TLR4 signaling pathway has a vital role in various physiological and pathological processes, including CCl_4-induced liver injury. It has been demonstrated that TLR4 recruits specific adaptor molecules, including MyD88, to initiate down-streaming signaling events towards the phosphorylation of NF-κB, thereby inducing the release of pro-inflammatory

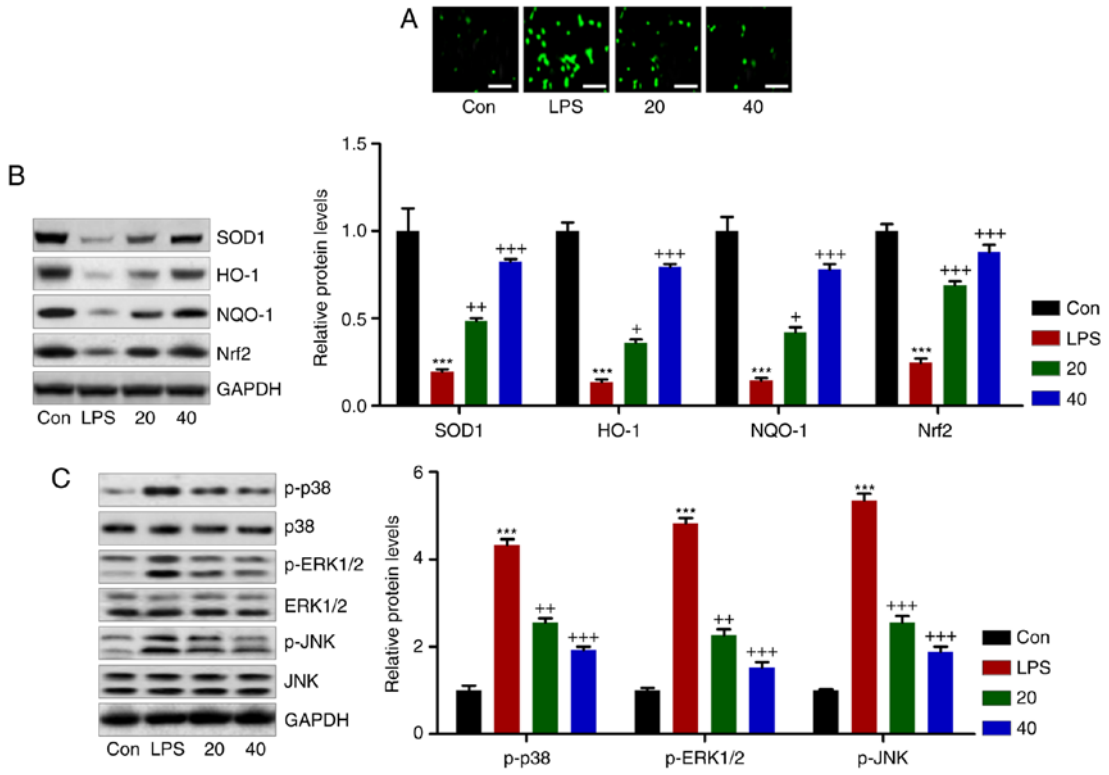

Figure 10. Breviscapine downregulates LPS-induced oxidative stress in L02 cells. (A) A 2',7'-dichlorofluorescein-diacetate assay was performed to measure the generation of reactive oxygen species in L02 cells treated with LPS with or without breviscapine treatment (20 or 40 μM). Scale bar, 50 μm. (B) SOD1, NQO-1, HO-1 and Nrf2, as well as (C) p-p38, p-ERK1/2 and p-JNK protein levels were measured using western blot analysis. The quantified results are provided in the bar graphs. Values are expressed as the mean ± standard error of the mean (n=10). ***P<0.001 vs. Con. $^{+}$P<0.05, $^{++}$P<0.01 and $^{+++}$P<0.001 vs. LPS group. Con, control; LPS, lipopolysaccharide; SOD, superoxide dismutase; HO-1, heme oxygenase 1; NQO-1, NAD(P)H quinone dehydrogenase 1; p-ERK, phosphorylated extracellular signal-regulated kinase; JNK, c-Jun N-terminal kinase; Nrf2, nuclear factor erythroid 2-related factor 2.

cytokines (42,43). In addition, NF-κB has a central role in the inflammatory response and triggers the expression of crucial inflammatory genes. Furthermore, NF-κB is one of the key transcription factors in LPS-stimulated inflammation, which regulates various inflammatory mediators, including TNF-α, IL-18, IL-6 and IL-1β (44). The IKK complex is activated by LPS through the TLR4 signaling pathway and phosphorylates IκBα in the cytoplasm. Consequently, it undergoes proteasomal degradation, leading to NF-κB release from the IKK complex and its translocation into the nucleus to subsequently enhance the expression of targeting genes involved in the inflammatory response (45,46). Thus, downregulation of the NF-κB signaling pathway regulated by TLR4/MyD88 is one of the major targets to attenuate the inflammatory response and associated diseases. Similarly, the present study indicated that the TLR4/MyD88 signaling pathway was activated *in vitro* and *in vivo* by LPS or CCl_4. Accordingly, the phosphorylation of IKKα, IκBα and NF-κB was stimulated, contributing to the secretion of pro-inflammatory cytokines. Breviscapine obviously exerted a suppressive effect on the TLR4/NF-κB signaling pathway, which appears to be a major mechanism of its anti-inflammatory action.

Apoptosis is a process that is tightly regulated by specific genes, including several pro- and anti-apoptotic genes expressing homologous proteins of the Bcl-2 family, including Bcl-2 and Bax, which are known to have an important role in determining whether a cell undergoes apoptosis (47-50). Apoptosis may be induced via the mitochondrial pathway and the Bcl-2/Bax equilibrium regulates the mitochondrial apoptotic pathway (51). Bax is a typical pro-apoptotic protein in the cytosol, which may translocate to the mitochondria to induce apoptosis, while Bcl-2 is an anti-apoptotic protein that suppresses Bax-induced apoptosis (52). Bax activation stimulates caspase-3 and PARP cleavage through Apaf-1 stimulation. Consequently, the apoptotic response is induced, eventually leading to cell death (53,54). Western blot analysis indicated that Bax expression in the CCl_4-treated mice was upregulated compared with that in the control group, whereas Bcl-2 expression in the CCl_4-treated group was downregulated. Of note, co-treatment with breviscapine inhibited the increase of Bax expression and the decrease of Bcl-2 expression induced by CCl_4. Consequently, the higher caspase-3 and PARP cleavage caused by CCl_4 was suppressed by breviscapine administration. Therefore, these results indicated that breviscapine ameliorated CCl_4-induced liver cell apoptosis by modulating the expression of the apoptosis-associated molecules Bax and Bcl-2 to inhibit the caspase-3-dependent apoptotic signaling pathway. To the best of our knowledge, the present study was the first to indicate that breviscapine alleviates liver injury through suppression of apoptosis and oxidative stress. According to previous studies, an interaction between apoptosis and inflammation is involved in regulating the progression and development of various types of tumor (55,56). NF-κB is generally considered to be a survival factor that activates the expression of various anti-apoptotic genes, including Bcl-2, myeloid leukemia-1, Bcl extra-large protein and cellular (FADD-like IL-1β-converting

enzyme)-inhibitory protein. Inhibition of NF-κB leads to downregulation of the NF-κB-regulated anti-apoptotic proteins, thereby promoting apoptotic cell death (57,58). As activation of NF-κB is a frequent event in cancer cells, it may be an attractive potential therapeutic target. However, NF-κB inhibition alone is not sufficient to induce apoptosis (59).

The elevation of cellular ROS is thought to cause various diseases and conditions, including diabetes, cardiovascular diseases, cancer and aging (60-62). CCl_4 causes severe liver cell damage via elevation of ROS, leading to necrosis and apoptosis to result in acute liver injury. It is evident that direct reduction of ROS levels and inhibition of the CCl_4-induced oxidative chain reaction are critical for the prevention and treatment of CCl_4-induced acute liver damage (63). Therefore, supplementation with anti-oxidants is beneficial for human health. According to a previous study, breviscapine exerted anti-oxidant effects in the livers of rats (64). The present study indicated that breviscapine reduced oxidative stress via enhancing anti-oxidants, including SOD1, NQO-1, HO-1 and Nrf2. ROS may affect the activity of MAPKs (p38, ERK1/2 and JNK), which are involved in important signaling pathways regulating cell proliferation, differentiation and death in response to a variety of stimuli. MAPKs also sense the cellular redox status and are common targets for ROS (34,35,65,66). In the present study, breviscapine de-activated MAPK signaling induced by CCl_4 and LPS *in vivo* and *in vitro*, respectively. Therefore, the breviscapine-mediated attenuation of liver injury was also linked to its suppression of oxidative stress, which was in line with the results of a previous study (67).

In conclusion, the present study indicated the potential protective effects of breviscapine against CCl_4-induced liver damage. The hepatoprotective effects of breviscapine depend on its ability to reduce the generation of ROS, as well as pro-inflammatory signalling and apoptosis through de-activation of TLR4/NF-κB, caspase-3/PARP and MAPK signaling. Overall, the present study provides evidence for the protective effects of breviscapine against CCl_4-induced liver injury and suggests breviscapine as a potential hepatoprotective agent to prevent oxidative liver damage.

Acknowledgements

Not applicable.

Funding

This work was supported by the Institutional Animal Care and Use Committee of the Beijing Chao-Yang Hospital (Beijing, China) (grant no. Yt20115713c).

Availability of data and materials

The datasets generated and analyzed in the present study are included in this published article.

Authors' contributions

YL, PW, XZ and YD contributed to the design of this study and performed the experiments. QH drafted the manuscript. All the authors read and approved the final manuscript.

Ethics and consent to participate

This work was approved by the Institutional Animal Care and Use Committee of the Beijing Chao-Yang Hospital (Beijing, China). The present study was conducted following the Guide for the Care and Use of Experimental Animals of the National Institutes of Health (NIH) from 1996 (20).

Consent for publication

Not applicable.

Competing interests

The authors declare that they have no competing interests.

References

1. Rowland A, Miners JO and Mackenzie PI: The UDP-glucuronosyltransferases: Their role in drug metabolism and detoxification. Int J Biochem Cell Biol 45: 1121-1132, 2013.
2. Mao S, Gao D, Liu W, Wei H and Lin JM: Imitation of drug metabolism in human liver and cytotoxicity assay using a microfluidic device coupled to mass spectrometric detection. Lab Chip 12: 219-226, 2012.
3. Dawson S, Stahl S, Paul N, Barber J and Kenna JG: In vitro inhibition of the bile salt export pump correlates with risk of cholestatic drug-induced liver injury in humans. Drug Metab Dispos 40: 130-138, 2012.
4. Huang HL, Wang YJ, Zhang QY, Liu B, Wang FY, Li JJ and Zhu RZ: Hepatoprotective effects of baicalein against CCl_4-induced acute liver injury in mice. World J Gastroenterol 18: 6605-6613, 2012.
5. Chen X, Meng Q, Wang C, Liu Q, Sun H, Huo X, Sun P, Yang X, Peng J and Liu K: Protective effects of calycosin against CCl_4-induced liver injury with activation of FXR and STAT3 in mice. Pharm Res 32: 538-548, 2015.
6. Chen X, Gong X, Jiang R, Wang B, Kuang G, Li K and Wan J: Resolvin D1 attenuates CCl_4-induced acute liver injury involving up-regulation of HO-1 in mice. Immunopharmacol Immunotoxicol 38: 61-67, 2016.
7. Perugorria MJ, Sharif O, Oakley F, Esparza-Baquer A, Korosec A, Mann J, Labiano I, Tiniakos D, Gawish R, Jiménez-Agüero R, *et al*: TREM-2 protects the liver from immune-mediated hepatocellular damage. J Hepatol 64: S133-S158, 2016.
8. Karkampouna S, Goumans MJ, Ten Dijke P, Dooley S and Kruithof-de Julio M: Inhibition of TGFβ type I receptor activity facilitates liver regeneration upon acute CCl_4 intoxication in mice. Arch Toxicol 90: 347-357, 2016.
9. Liu J, Wang X, Liu R, Liu Y, Zhang T, Fu H and Hai C: Oleanolic acid co-administration alleviates ethanol-induced hepatic injury via Nrf-2 and ethanol-metabolizing modulating in rats. Chem Biol Interact 221: 88-98, 2014.
10. Bansal R, Nagórniewicz B, Storm G and Prakash J: PS-072-Relaxin-coated superparamagnetic iron-oxide nanoparticles as a novel theranostic approach for the diagnosis and treatment of liver fibrosis. J Hepatol 66: S33-S62, 2017.
11. Navarro VJ, Barnhart H, Bonkovsky HL, Davern T, Fontana RJ, Grant L, Reddy KR, Seeff LB, Serrano J, Sherker AH, *et al*: Liver injury from herbals and dietary supplements in the US drug-induced liver injury network. Hepatology 60: 1399-1408, 2014.
12. Salomone F, Godos J and Zelber-Sagi S: Natural antioxidants for non-alcoholic fatty liver disease: Molecular targets and clinical perspectives. Liver Int 36: 5-20, 2016.
13. Wang X, Xia H, Liu Y, Qiu F and Di X: Simultaneous determination of three glucuronide conjugates of scutellarein in rat plasma by LC-MS/MS for pharmacokinetic study of breviscapine. J Chromatogr B Analyt Technol Biomed Life Sci 965: 79-84, 2014.
14. Zhao Y, Ma X, Wang J, He X, Zhang Y, Wang Y, Liu H, Shen H and Xiao X: A system review of anti-fibrogenesis effects of compounds derived from chinese herbal medicine. Mini Rev Med Chem 16: 163-175, 2016.

15. Qian LH, Li NG, Tang YP, Zhang L, Tang H, Wang ZJ, Liu L, Song SL, Guo JM and Ding AW: Synthesis and bio-activity evaluation of scutellarein as a potent agent for the therapy of ischemic cerebrovascular disease. Int J Mol Sci 12: 8208-8216, 2011.
16. Zeng J and Cai S: Breviscapine suppresses the growth of non-small cell lung cancer by enhancing microRNA-7 expression. J Biosci 42: 121-129, 2017.
17. Wu Y, Fan Q, Lu N, Tao L, Gao Y, Qi Q and Guo Q: Breviscapine-induced apoptosis of human hepatocellular carcinoma cell line HepG2 was involved in its antitumor activity. Phytother Res 24: 1188-1194, 2010.
18. Jiang L, Xia QJ, Dong XJ, Hu Y, Chen ZW, Chen K, Wang KH, Liu J and Wang TH: Neuroprotective effect of breviscapine on traumatic brain injury in rats associated with the inhibition of GSK3β signaling pathway. Brain Res 1660: 1-9, 2017.
19. He X, Long W, Dong H, Wang C, Chu X, Zheng Q and Fan S: Evaluation of the protective effects of 13 traditional Chinese medicine compounds on ionizing radiation injury: Bupleurum, shenmai, and breviscapine as candidate radioprotectors. RSC Adv 7: 22640-22648, 2017.
20. Clark JD, Gebhart GF, Gonder JC, Keeling ME and Kohn DF: Special Report: The 1996 guide for the care and use of laboratory animals. ILAR J 38: 41-48, 1997.
21. Andrade-Cetto A and Wiedenfeld H: Anti-hyperglycemic effect of opuntia streptacantha lem. J Ethnopharmacol 133: 940-943, 2011.
22. Wang Y: Attenuation of berberine on lipopolysaccharide-induced inflammatory and apoptosis responses in β-cells via TLR4-independent JNK/NF-κB pathway. Pharm Biol 2013.
23. Liang CJ, Lee CW, Sung HC, Chen YH, Wang SH, Wu PJ, Chiang YC, Tsai JS, Wu CC, Li CY and Chen YL: Magnolol reduced TNF-α-induced vascular cell adhesion molecule-1 expression in endothelial cells via JNK/p38 and NF-κB signaling pathways. Am J Chin Med 42: 619-637, 2014.
24. Xu MX, Wang M and Yang WW: Gold-quercetin nanoparticles prevent metabolic endotoxemia-induced kidney injury by regulating TLR4/NF-κB signaling and Nrf2 pathway in high fat diet fed mice. Int J Nanomedicine 12: 327-345, 2017.
25. Uesugi T, Froh M, Arteel GE, Bradford BU and Thurman RG: Toll-like receptor 4 is involved in the mechanism of early alcohol-induced liver injury in mice. Hepatology 34: 101-108, 2001.
26. Li JM, Ge CX, Xu MX, Wang W, Yu R, Fan CY and Kong LD: Betaine recovers hypothalamic neural injury by inhibiting astrogliosis and inflammation in fructose-fed rats. Mol Nutr Food Res 59: 189-202, 2015.
27. Kluk MJ, Chapuy B, Sinha P, Roy A, Dal Cin P, Neuberg DS, Monti S, Pinkus GS, Shipp MA and Rodig SJ: Immunohistochemical detection of MYC-driven diffuse large B-cell lymphomas. PloS One 7: e33813, 2012.
28. Xu MX, Zhu YF, Chang HF and Liang Y: Nanoceria restrains PM2.5-induced metabolic disorder and hypothalamus inflammation by inhibition of astrocytes activation related NF-κB pathway in Nrf2 deficient mice. Free Radic Biol Med 99: 259-272, 2016.
29. Livak KJ and Schmittgen TD: Analysis of relative gene expression data using real-time quantitative PCR and the 2(-Delta Delta C(T)) method. Methods 25: 402-408, 2001.
30. Tewari R, Choudhury SR, Ghosh S, Mehta VS and Sen E: Involvement of TNFα-induced TLR4-NF-κB and TLR4-HIF-1α feed-forward loops in the regulation of inflammatory responses in glioma. J Mol Med (Berl) 90: 67-80, 2012.
31. Brentnall M, Rodriguez-Menocal L, De Guevara RL, Cepero E and Boise LH: Caspase-9, caspase-3 and caspase-7 have distinct roles during intrinsic apoptosis. BMC Cell Biol 14: 32, 2013.
32. Cichoż-Lach H and Michalak A: Oxidative stress as a crucial factor in liver diseases. World J Gastroenterol 20: 8082-8091, 2014.
33. Sutti S, Jindal A, Locatelli I, Vacchiano M, Gigliotti L, Bozzola C and Albano E: Adaptive immune responses triggered by oxidative stress contribute to hepatic inflammation in NASH. Hepatology 59: 886-897, 2014.
34. Cordero-Herrera I, Martín MA, Goya L and Ramos S: Cocoa flavonoids protect hepatic cells against high-glucose-induced oxidative stress: Relevance of MAPKs. Mol Nutr Food Res 59: 597-609, 2015.
35. Ma JQ, Ding J, Zhang L and Liu CM: Ursolic acid protects mouse liver against CCl 4-induced oxidative stress and inflammation by the MAPK/NF-κB pathway. Environ Toxicol Pharmacol 37: 975-983, 2014.
36. Luyendyk JP, Kassel KM, Allen K, Guo GL, Li G, Cantor GH and Copple BL: Fibrinogen deficiency increases liver injury and early growth response-1 (Egr-1) expression in a model of chronic xenobiotic-induced cholestasis. Am J Pathol 178: 1117-1125, 2011.
37. Esmaeili MA and Alilou M: Naringenin attenuates CCl_4-induced hepatic inflammation by the activation of an Nrf2-mediated pathway in rats. Clin Exp Pharmacol Physiol 41: 416-422, 2014.
38. Wang Y, Lian F, Li J, Fan W, Xu H, Yang X, Liang L, Chen W and Yang J: Adipose derived mesenchymal stem cells transplantation via portal vein improves microcirculation and ameliorates liver fibrosis induced by CCl_4 in rats. J Transl Med 10: 133, 2012.
39. Pöling J, Gajawada P, Richter M, Lörchner H, Polyakova V, Kostin S, Shin J, Boettger T, Walther T, Rees W, *et al*: Therapeutic targeting of the oncostatin M receptor-β prevents inflammatory heart failure. Basic Res Cardiol 109: 396, 2014.
40. Szpechcinski A, Chorostowska-Wynimko J, Struniawski R, Kupis W, Rudzinski P, Langfort R, Puscinska E, Bielen P, Sliwinski P and Orlowski T: Cell-free DNA levels in plasma of patients with non-small-cell lung cancer and inflammatory lung disease. Br J Cancer 113: 476-483, 2015.
41. Shi H, Dong L, Jiang J, Zhao J, Zhao G, Dang X, Lu X and Jia M: Chlorogenic acid reduces liver inflammation and fibrosis through inhibition of toll-like receptor 4 signaling pathway. Toxicology 303: 107-114, 2013.
42. Zhu HT, Bian C, Yuan JC, Chu WH, Xiang X, Chen F, Wang CS, Feng H and Lin JK: Curcumin attenuates acute inflammatory injury by inhibiting the TLR4/MyD88/NF-κB signaling pathway in experimental traumatic brain injury. J Neuroinflammation 11: 59, 2014.
43. Ma Y, He M and Qiang L: Exercise therapy downregulates the overexpression of TLR4, TLR2, MyD88 and NF-κB after cerebral ischemia in rats. Int J Mol Sci 14: 3718-3733, 2013.
44. Wang WY, Tan MS, Yu JT and Tan L: Role of pro-inflammatory cytokines released from microglia in Alzheimer's disease. Ann Transl Med 3: 136, 2015.
45. Wei HY and Ma X: Tamoxifen reduces infiltration of inflammatory cells, apoptosis and inhibits IKK/NF-kB pathway after spinal cord injury in rats. Neurol Sci 35: 1763-1768, 2014.
46. Baldwin AS: Regulation of cell death and autophagy by IKK and NF-κB: Critical mechanisms in immune function and cancer. Immunol Rev 246: 327-345, 2012.
47. Czabotar PE, Lessene G, Strasser A and Adams JM: Control of apoptosis by the BCL-2 protein family: Implications for physiology and therapy. Nat Rev Mol Cell Biol 15: 49-63, 2014.
48. Shirali S, Aghaei M, Shabani M, Fathi M, Sohrabi M and Moeinifard M: Adenosine induces cell cycle arrest and apoptosis via cyclinD1/Cdk4 and Bcl-2/Bax pathways in human ovarian cancer cell line OVCAR-3. Tumor Biol 34: 1085-1095, 2013.
49. Sun Y, Lin Y, Li H, Liu J, Sheng X and Zhang W: 2,5-Hexanedione induces human ovarian granulosa cell apoptosis through BCL-2, BAX, and CASPASE-3 signaling pathways. Arch Toxicol 86: 205-215, 2012.
50. Lee JS, Jung WK, Jeong MH, Yoon TR and Kim HK: Sanguinarine induces apoptosis of HT-29 human colon cancer cells via the regulation of Bax/Bcl-2 ratio and caspase-9-dependent pathway. Int J Toxicol 31: 70-77, 2012.
51. Hoshyar R, Bathaie SZ and Sadeghizadeh M: Crocin triggers the apoptosis through increasing the Bax/Bcl-2 ratio and caspase activation in human gastric adenocarcinoma, AGS, cells. DNA Cell Biol 32: 50-57, 2013.
52. Spampanato C, De Maria S, Sarnataro M, Giordano E, Zanfardino M, Baiano S, Cartenì M and Morelli F: Simvastatin inhibits cancer cell growth by inducing apoptosis correlated to activation of Bax and down-regulation of BCL-2 gene expression. Int J Oncol 40: 935-941, 2012.
53. Ouyang L, Shi Z, Zhao S, Wang FT, Zhou TT, Liu B and Bao JK: Programmed cell death pathways in cancer: A review of apoptosis, autophagy and programmed necrosis. Cell Prolif 45: 487-498, 2012.
54. Roos WP and Kaina B: DNA damage-induced cell death: From specific DNA lesions to the DNA damage response and apoptosis. Cancer Lett 332: 237-248, 2013.
55. Jost PJ and Ruland J: Aberrant NF-kappaB signaling in lymphoma: Mechanisms, consequences, and therapeutic implications. Blood 109: 2700-2707, 2007.
56. Dutta J, Fan Y, Gupta N, Fan G and Gélinas C: Current insights into the regulation of programmed cell death by NF-kappaB. Oncogene 25: 6800-6816, 2006.

57. Fujioka S, Sclabas GM, Schmidt C, Niu J, Frederick WA, Dong QG, Abbruzzese JL, Evans DB, Baker C and Chiao PJ: Inhibition of constitutive NF-kappa B activity by I kappa B alpha M suppresses tumorigenesis. Oncogene 22: 1365-1370, 2003.
58. Rogers R, Ouellet G, Brown C, Moyer B, Rasoulpour T and Hixon M: Cross-talk between the akt and nf-κb signaling pathways inhibits mehp-induced germ cell apoptosis. Toxicol Sci 106: 497-508, 2008.
59. Gasparian AV, Yao YJ, Kowalczyk D, Lyakh LA, Karseladze A, Slaga TJ and Budunova IV: The role of IKK in constitutive activation of NF-κB transcription factor in prostate carcinoma cells. J Cell Sci 115: 141-151, 2002.
60. Harrison DG, Cai H, Landmesser U and Griendling KK: Interactions of angiotensin II with NAD(P)H oxidase, oxidant stress and cardiovascular disease. J Renin Angiotensin Aldosterone Syst 4: 51-61, 2003.
61. Inoguchi T, Sonta T, Tsubouchi H, Etoh T, Kakimoto M, Sonoda N, Sato N, Sekiguchi N, Kobayashi K, Sumimoto H, *et al*: Protein kinase C-dependent increase in reactive oxygen species (ROS) production in vascular tissues of diabetes: Role of vascular NAD(P)H oxidase. J Am Soc Nephrol 14 (Suppl 3): S227-S232, 2003.
62. Singh KK: Mitochondrial dysfunction is a common phenotype in aging and cancer. Ann NY Acad Sci 1019: 260-264, 2004.
63. Ulicná O, Greksák M, Vancová O, Zlatos L, Galbavý S, Bozek P and Nakano M: Hepatoprotective effect of rooibos tea (Aspalathus linearis) on CCl 4-induced liver damage in rats. Physiol Res 52: 461-466, 2003.
64. Wu YG, Xia LL, Lin H, Zhou D, Qian H and Lin ST: Prevention of early liver injury by breviscapine in streptozotocin-induced diabetic rats. Planta Med 73: 433-438, 2007.
65. Son Y, Cheong YK, Kim NH, Chung HT, Kang DG and Pae HO: Mitogen-activated protein kinases and reactive oxygen species: How can ROS activate MAPK pathways? J Signal Transduct 2011: 792639, 2011.
66. Sauer H, Wartenberg M and Hescheler J: Reactive oxygen species as intracellular messengers during cell growth and differentiation. Cell Physiol Biochem 11: 173-186, 2001.
67. Lin YZ, Lu ZY, Liang XH, Li K, Peng B and Gong J: Effect of breviscapine against hepatic ischemia reperfusion injury. J Surg Res 203: 268-274, 2016.